Eur. Phys. J. Plus (2019) **134**: 89
DOI 10.1140/epjp/i2019-12497-1

THE EUROPEAN PHYSICAL JOURNAL PLUS

Review

Introduction to experimental nuclear astrophysics*

A. Formicola[1,a] and G. Imbriani[2]

[1] INFN, Laboratori Nazionali del Gran Sasso, Assergi, via Acitelli 22, 67100 L'Aquila, Italy
[2] Dipartimento Fisica "E. Pancini", Università degli Studi Napoli "Federico II" and INFN, Napoli, Italy

Received: 13 June 2018 / Revised: 3 December 2018
Published online: 7 March 2019
© Società Italiana di Fisica / Springer-Verlag GmbH Germany, part of Springer Nature, 2019

Abstract. The present contribution aims to present some general features of the experimental approaches in Nuclear Astrophysics. After a general introduction on light elements nucleosynthesis and on how to determine the reaction rates in a stellar environment, we will focus our attention on underground experiments aimed to directly measure nuclear cross sections of astrophysics interest. We will discuss the $^{14}N(p,\gamma)^{15}O$ and $^{12}C + {}^{12}C$ reactions, underlying the advantages in approaching these measurements in a deep underground laboratory, as the Laboratori Nazionali del Gran Sasso.

1 Introduction

The detailed description of most astrophysical and cosmological scenarios requires an accurate knowledge of the many relevant nuclear processes involved, *i.e.* amount of baryonic matter in the Universe, solar neutrino fluxes, novae and supernovae explosions, gamma rays fluxes, etc. Nuclear fusion reactions are at the heart of nuclear astrophysics as they determine the nucleosynthesis of the elements in the earliest stages of the universe and in all the objects formed thereafter, and control the energy generation, neutrino luminosity, and evolution of stars. An accurate and precise knowledge of the cross section of these reactions is thus essential to describe the evolution of the universe. Since most of the cross sections at the astrophysical relevant energies are too small to be directly measured in a laboratory, they need to be extrapolated through models on the basis of the existing experimental data at higher energies [1]. In many cases, because of the difficulty of taking into account all of the complexity of the nuclear structure, the accuracy reached by extrapolation is not sufficient to obtain unambiguous results from models. Improved measurements on a wide range of energies are needed to reduce the uncertainty of the extrapolations. Alternative approaches is to use indirect methods to study some key nuclear parameters, such as, for example, trojan horse [2].

Coming back to the direct measurement approach, low-energy studies of thermonuclear reactions in a laboratory at the earth's surface are hampered by several sources of background, *i.e.* cosmic rays, environmental radioactivity and beam target impurity induced nuclear reactions. In this manuscript, we will focus our attention on the attempts to reduce background induced by cosmic rays in the detectors, which leads typically to more than 10 events per hour in common detectors. Conventional passive or active shielding around the detectors can only partially reduce the problem. The best solution so far was to install an accelerator facility in a deep underground laboratory, in a similar way to solar neutrino detectors. In the case of National Laboratory of Gran Sasso the 1400 m of rock above the laboratory halls leads to a reduction of the muon flux, the most penetrating component of the cosmic-rays, by a factor 10^6 with respect to the Earth's surface [3]. Several cross sections belonging to the hydrogen burning have been studied in the framework of this unique project, called LUNA (Laboratory for Underground Nuclear Astrophysics), that was initiated almost 20 years ago. Some results achieved and their impact on stellar evolution and nucleosynthesis modelling will be reviewed in the next sections [4].

2 Principles of stellar structure and evolution

How and where are stars born? Observational evidence points to the interstellar gas and dust clouds along the Galaxy's spiral arms as being the birthplace of stars. As some stars, such as those responsible for planetary nebulae, novae and supernovae, approach the end of their lives, they return some of their masses to the interstellar medium.

* Focus Point on "Rewriting Nuclear Physics Textbooks: Basic Nuclear Interactions and Their Link to Nuclear Processes in the Cosmos and on Earth" edited by N. Alamanos, C. Bertulani, A. Bonaccorso, A. Bracco, D. Brink, G. Casini, M. Taiuti.

[a] e-mail: formicola@lngs.infn.it

New generations of stars are thus always forming from the "ashes" of previous generations. The existence of interstellar matter, and its organization into clouds of up to several hundred thousand of solar masses, argues that the gas pressure in clouds is sufficient to balance the effect of gravity [5]. The first step in making new stars is to compress a cloud to strengthen gravity's effect so that cloud material can contract and fragment into smaller units that eventually collapse to form stars. A promising way of getting this process going is the travelling compression wave, or density wave, which astronomers believe is responsible for the Galaxy's spiral arm structure [6]. As the wave moves through a cool molecular cloud, it compresses the cloud, driving the particles closer together. Their mutual gravitational attraction is now greater than the gas pressure. If the compressed cloud has no other force that can halt contraction, collapse continues until the matter heats up, raising the gas pressure sufficiently to resist further contractions. Another possible mechanism for compressing molecular clouds is supernovae outburst: an expanding shock front on the leading edge of the gas shell expelled by a supernova outburst impinges on nearby clouds and compresses them by a factor of 10 or more, triggering therefore a gravitational collapse [5]. The discovery that some young clusters of stars are located inside the expanding shells of old supernova remnants certainly makes this a possible mechanism. Finally, the collapse of clouds could begin if a cloud was cooled so the gas pressure would decrease. There are several possible ways of cooling clouds, one possibility is dust grains radiating energy away in the form of infrared radiation [7]. Regardless of what starts the process, a fragmenting molecular cloud breaks into smaller units, and the fragments attract more matter and grow in mass. The rate at which stars are created from fragments of an interstellar cloud and the number of stars of different masses formed depends on several factors: total mass, density, temperature, magnetic fields, and the amount of internal motion stirring the material [7].

Matter in collapsing fragments converts its gravitational potential energy into thermal energy, some of which is radiated away into space as infrared radiation. As the gas becomes denser, the central regions of a forming star become opaque, therefore reducing the outward flow of radiation. The effect of this is to decrease the loss of energy so the temperature rises and the gas pressure increases. This causes the central region to slow down from a free fall collapse to a gradual contraction as it approaches a balance between gas pressure, which is pushing outward, and the force of gravity, which is pushing inward. Now the "embryo" star appears on the Hertzsprung-Russell (H-R) diagram (in which one plots the surface T *versus* the luminosity of a star) for the first time. The evolution starts on the coldest fringes of the diagram on evolutionary tracks determined from stellar models: it is a protostar. The temperature of a protostar's surface is about 4000 K, and energy in its deep interior is transported to the surface entirely by convection, from the center to the surface. In this slower-contraction phase, a protostar decreases its luminosity but keeps about the same surface temperature. Gravitational contractions eventually raise the temperature in a protostar's core to around 1 million K, which is hot enough to destroy light nuclei such as deuterium, lithium, beryllium, and boron (initially present in small quantities) by nuclear reactions. These are the first stages of the star's thermonuclear existence, from which it derives a small amount of energy. The next stage is to initiate hydrogen burning if the mass of the gas cloud exceed 0.1 $M_\odot$ ($M_\odot$ is the solar mass). By the time the protostar's central temperature has risen to several million degrees, the hydrogen burning begins to supply some luminosity. Several million years later the protostar arrives on the zero-age main sequence in the H-R diagram, where hydrogen burning supplies 100% of the luminosity. Astronomers define the zero-age Main Sequence as the line along which protostars of different masses cease to contract and derive all their luminosity from hydrogen burning. The protostar is now a full star. During hydrogen burning, the hydrogen core is slowly replaced by a helium core: if the mass of the star is larger than about 2 $M_\odot$, when hydrogen at the center is exhausted, there is hydrogen to helium conversion only in a shell around a depleted central core. The hydrogen shell burning is then the main source of energy, and the helium core slowly increases in mass while the burning shell moves outward converting more hydrogen into helium. The massive core has heated up through contraction to a temperature at which helium can be converted into carbon. In a similar way, heavier elements are generated and can undergo a core nuclear burning process, provided the star mass is large enough, while new shells are formed. The sequence of stellar burning terminates when the core of the star is largely composed of stable nuclei with $A \leq 56$. In fact, elements beyond iron, involved in nuclear reactions, require energy to occur. As soon as there is insufficient internal energy being produced, the core cannot support the outer layers against gravitational collapse and the star begins its final contraction. A large amount of gravitational potential energy is converted into kinetic energy and the star becomes a supernova (so-called type-II supernova) and a large fraction of its mass is thrown out into space. From the point of view of nucleosynthesis, this phase is very important, because there will be a large amount of neutron available, which may be easily captured building isotopes heavier the iron, *i.e.* r-process.

3 Nuclear networks

3.1 H-burning: the p-p chain and the CNO cycle

The hydrogen burning phase is initiated when the centre of a start reaches a temperature of about 6 MK and the proton-proton reaction can efficiently synthesis deuterium. In the hydrogen rich environment the deuterium reacts almost instantly with another proton producing ^{3}He, which in turn forms, together with another ^{3}He nucleus, an

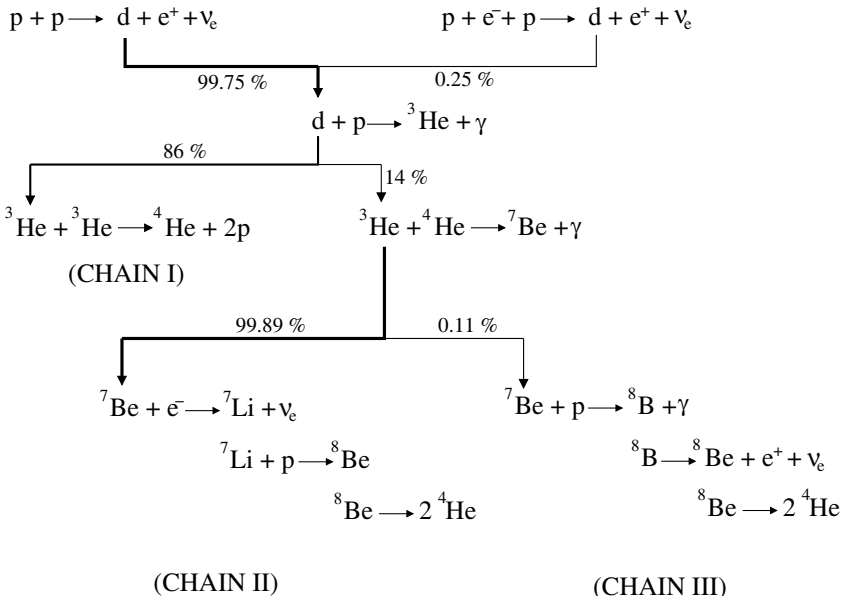

Fig. 1. The p-p chain.

α-particle and releases two protons through the ^{3}He(^{3}He, 2p)^{4}He. This represents the way in the core of a star 4 protons may be converted in a helium nucleus (p-p chain). There is actually another nuclear network having the same final results, whose name is CNO cycle. We can synthesise the effect of p-p chains and CNO cycle as follows:

$$4\mathrm{p} \longrightarrow {}^4\mathrm{He} + 2e^+ + 2\nu + 26.73\,\mathrm{MeV}. \tag{1}$$

The sequence of reactions for the p-p chain is shown in fig. 1; a first possibility is the proton-proton reaction: p(p, $e^+\nu$)d is the slowest reaction, and therefore represents the rate-limiting step for the whole chain. The cross section for this reaction is too small to be measured in a laboratory today, so it is calculated from standard weak-interaction theory to be on the order 10^{-33} b at keV energies and 10^{-23} b at MeV energies [8]. When the center of the star reaches a temperature of $T \approx 6 \cdot 10^6$ K the chains I and II become more significant, the reaction $^3\mathrm{He} + {}^3\mathrm{He}$ produces a ^{4}He nucleus and two protons (chain I):

$$^3\mathrm{He} + {}^3\mathrm{He} \rightarrow {}^4\mathrm{He} + \mathrm{p} + \mathrm{p}. \tag{2}$$

An alternative is to encounter an α-particle,

$$^3\mathrm{He} + {}^4\mathrm{He} \rightarrow {}^7\mathrm{Be} + \gamma. \tag{3}$$

^{7}Be is unstable and decays via electron capture to ^{7}Li and a neutrino of either 0.38 MeV or 0.86 MeV. The ^{7}Li captures a proton producing ^{8}Be, which decays producing two helium nuclei (chain II).

The ^{7}Be electron capture competes with proton capture producing ^{8}B, which decays to ^{8}Be producing a positron, a high energy neutrino (0 MeV $\leq E_\nu \leq$ 15 MeV), and again two helium nuclei (chain III).

The complete processes are indicated schematically in fig. 1. Since, however, the energy lost via neutrino emission depends on the specific chain, we must consider three different Q-values, corresponding to the 3 chains:

$$\text{p-p chain} \begin{cases} \mathrm{p} - \mathrm{p} - I \rightarrow Q_{\mathrm{eff}} = 26.2\,\mathrm{MeV}, \\ \mathrm{p} - \mathrm{p} - II \rightarrow Q_{\mathrm{eff}} = 25.66\,\mathrm{MeV}, \\ \mathrm{p} - \mathrm{p} - III \rightarrow Q_{\mathrm{eff}} = 19.17\,\mathrm{MeV}. \end{cases}$$

If, in addition to hydrogen and helium, there are heavier elements present in the interior of a star, a second possibility for the conversion of hydrogen into helium is offered by a reaction cycle investigated in late 30s of last century by Bethe and von Weizsäker [9,10]: the CNO cycle. In this cycle, the elements carbon, nitrogen, and oxygen (C, N, O) are involved but are quantitatively "returned" at the end, due to the fact that they are "catalysts" in each single cycle (see fig. 2).

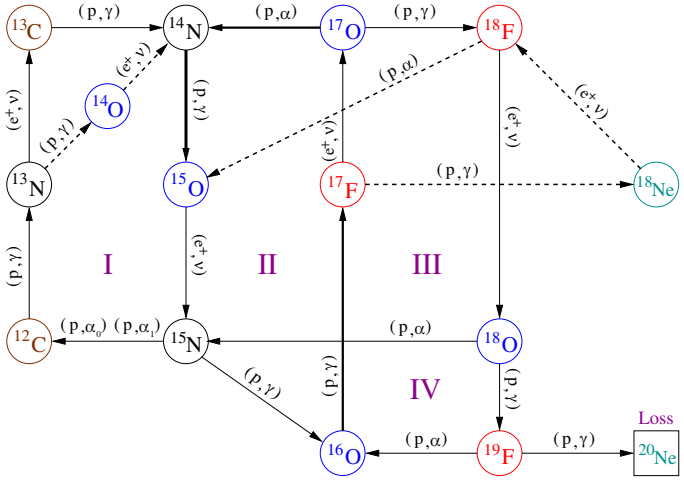

Fig. 2. The CNO cycle. Thicknesses of lines are inversely proportional to the reaction rate, dotted lines correspond to hot CNO.

When the central temperature increases to $T_c \approx 15 \cdot 10^6\,\mathrm{K}$, the present carbon in the star can react with the sea of protons producing ^{13}N, which decays to ^{13}C which, in turn, captures another proton. As shown in eq. (4), at the end of this first part of the CNO-I cycle four protons are transformed in one helium nucleus, exactly as in the p-p chain and with the same Q-value:

$$\text{CNO-I} \begin{cases} {}^{12}\mathrm{C} + \mathrm{p} \rightarrow {}^{13}\mathrm{N} + \gamma, \\ {}^{13}\mathrm{N} \rightarrow {}^{13}\mathrm{C} + e^+ + \nu, \\ {}^{13}\mathrm{C} + \mathrm{p} \rightarrow {}^{14}\mathrm{N} + \gamma, \\ {}^{14}\mathrm{N} + \mathrm{p} \rightarrow {}^{15}\mathrm{O} + \gamma, \\ {}^{15}\mathrm{O} \rightarrow {}^{15}\mathrm{N} + e^+ + \nu, \\ {}^{15}\mathrm{N} + \mathrm{p} \rightarrow {}^{12}\mathrm{C} + \alpha. \end{cases} \tag{4}$$

Network calculations show that the reaction $^{14}\mathrm{N}(\mathrm{p},\gamma)^{15}\mathrm{O}$ determines the rate of the CNO cycle [11].

3.2 Helium burning

When all the hydrogen available in the centre is converted into helium, the core of the star starts to contract increasing the temperature, while the envelope of the star expands generating a Red Giant stars. If the mass of the star is large enough, when T_C exceeds 10^8 K the fusion of two α-particles can be followed by the capture of another α-particle, before ^{8}Be decays. This is the first reaction of helium burning and it can be interpreted as a three-body reaction between 3α nuclei, because of the very short life time of ^{8}Be. The carbon produced by this reaction can capture another α-particle forming an oxygen nucleus. The $^{12}\mathrm{C}(\alpha,\gamma)^{16}\mathrm{O}$ is, together to the triple-α reaction, the most important process in the helium burning. In general, in the first part of helium burning, since the ^{12}C density is too low, the only active process is the triple-α reaction. In the last part of the helium burning the leading process is the $^{12}\mathrm{C}(\alpha,\gamma)^{16}\mathrm{O}$ reaction. The larger is the reaction rate of this reaction the larger is the helium burning time, because the Q-value of the two processes is very similar but the $^{12}\mathrm{C}(\alpha,\gamma)^{16}\mathrm{O}$ consumes only one α-particle instead of the 3 which are consumed by the 3α reaction. $^{12}\mathrm{C}(\alpha,\gamma)^{16}\mathrm{O}$ is a crucial reaction to understand the last stages of the stellar evolution (see fig. 3).

The complete set of reactions which take place during the helium burning are:

$$\text{He burning} \begin{cases} 3\alpha \rightarrow {}^{12}\mathrm{C} + \gamma, \\ {}^{12}\mathrm{C} + \alpha \rightarrow {}^{16}\mathrm{O} + \gamma, \\ {}^{16}\mathrm{O} + \alpha \rightarrow {}^{20}\mathrm{Ne} + \gamma, \\ {}^{20}\mathrm{Ne} + \alpha \rightarrow {}^{24}\mathrm{Mg} + \gamma, \\ {}^{24}\mathrm{Mg} + \alpha \rightarrow {}^{28}\mathrm{Si} + \gamma. \end{cases}$$

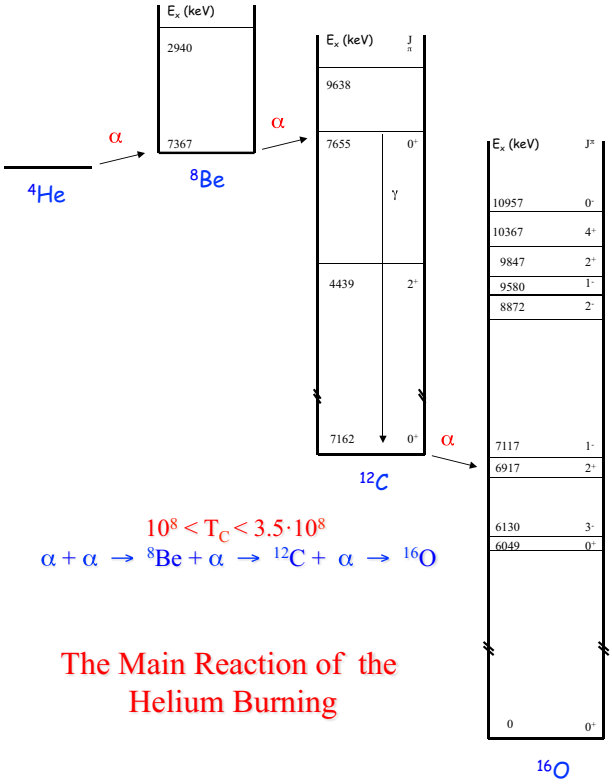

Fig. 3. The main reaction of helium burning with the nuclear levels of the particles involved, energy levels from *Table of Isotopes* (`http://www.nndc.bnl.gov/nudat2/`).

In addition to this main channel the α capture by ^{14}N is also possible, and a sequence of processes activate:

$$\begin{aligned} {}^{14}\mathrm{N} + \alpha &\rightarrow {}^{18}\mathrm{F} + \gamma, \\ {}^{18}\mathrm{F} + \beta^{+} &\rightarrow {}^{18}\mathrm{O} + \nu, \\ {}^{18}\mathrm{O} + \alpha &\rightarrow {}^{22}\mathrm{Ne} + \gamma, \\ {}^{22}\mathrm{Ne} + \alpha &\rightarrow {}^{25}\mathrm{Mg} + n, \\ &\rightarrow {}^{26}\mathrm{Mg} + \gamma. \end{aligned}$$

Note, by the way, that the process $^{22}\mathrm{Ne}(\alpha,\mathrm{n})^{25}\mathrm{Mg}$ is one of the main producers of neutrons.

At the end of the core helium burning the chemical composition of the exhausted core will be dominated by the C and O in a ratio which depends on the $^{12}\mathrm{C}(\alpha,\gamma)^{16}\mathrm{O}$ reaction rate plus a very small fraction of ^{20}Ne, ^{24}Mg and ^{28}Si.

3.3 Carbon and advanced burning

When the central temperature reaches $0.8 \cdot 10^9$ K the central carbon burning takes place. The carbon burning main reactions are:

$$\begin{aligned} {}^{12}\mathrm{C}({}^{12}\mathrm{C},\alpha)^{20}\mathrm{Ne} & \\ & {}^{23}\mathrm{Na}(\mathrm{p},\alpha)^{20}\mathrm{Ne} \\ & \nearrow \\ {}^{12}\mathrm{C}({}^{12}\mathrm{C},\mathrm{p})^{23}\mathrm{Na} & \\ & \searrow \\ & {}^{23}\mathrm{Na}(\mathrm{p},\gamma)^{24}\mathrm{Mg} \end{aligned}$$

At the end of burning, almost all of the carbon nuclei are transformed into ^{20}Ne, while only a small fraction of ^{24}Mg is produced. Note, however, that this fraction grows proportionally with the initial amount of ^{12}C.

Neon burning starts when T_C reaches about $1.2 \cdot 10^9$ K. The main reactions of neon burning are:

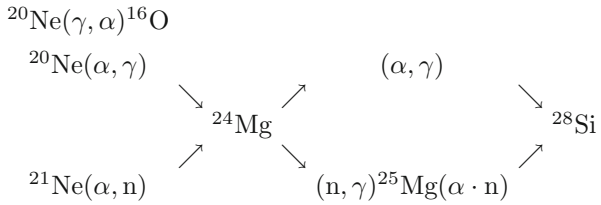

At the end of this burning, almost all the neon nuclei are transformed into oxygen with some amount of ^{24}Mg and ^{28}Si, which depend on the initial Ne abundance.

When the T_C raises above $2.5 \cdot 10^9$ K, oxygen burning starts. All the oxygen is transformed into ^{28}Si, ^{30}Si, ^{32}S and ^{34}S and its duration is about one year.

The last quiescent burning involves the silicon and it begins when $T_C \sim 3.5 \cdot 10^9$ K. The typical time-scale of this burning is of the order of the months. This last burning produces an iron core of almost 1.5 $M_\odot$.

Once the central temperature exceeds 5 billion degrees, the idea of "real" processes which change the chemical composition of the matter becomes meaningless. The matter settles in a condition called nuclear statistical equilibrium (NSE) in which all the (strong) direct and reverse reactions are at the equilibrium. Since the changing of the NSE distribution with the temperature requires the absorption of energy, indeed of a release, a collapse of the core starts. This collapse ends when the matter reaches the nuclear density; at this stage a rebound occurs which leads to a shock wave moving outward. In a very small time (less than 1 s) almost 10^{53} erg of energy are produced:

- 99% of the energy is lost via neutrinos;
- 0.99% (10^{51} erg) is used to expel the envelope;
- "only" 0.01% (10^{49} erg) are shined on as visible photons.

4 Overview of thermonuclear reactions in stars

Nuclear reactions are the "engine" which supplies the stellar "machine"; therefore, the understanding of stellar evolution largely depends on our knowledge on nuclear reaction rates. If we consider the strong interaction between nuclides $(1 + 2 \rightarrow 3 + 4)$, then, using energy conservation, the energy consumed or produced by the reaction is:

$$Q = (m_1 + m_2 - m_3 - m_4)c^2, \tag{5}$$

where Q is the Q-value in MeV and m_i (in amu) are the masses of the interacting particles. The main reactions in the stellar burnings, which involve particles lighter than iron, are esoenergetic ($Q > 0$). This occurrence allows stars to stop gravitational contraction, living in hydrostatic equilibrium and shining photons and neutrinos for such a long time.

To obtain the energy produced by nuclear reactions per second, the first step is to calculate the probability that a reaction takes place. This is proportional to the cross section σ. Considering N_X and N_Y particles per cubic centimeter of two differents species, which constitute the stellar gas, the number of reactions per cm^3 per s (reaction rate) is (X = projectile and Y = target):

$$r = N_X N_Y v\sigma(v), \tag{6}$$

where v is the relative velocity in cm/s. Introducing the effective cross section ($F = \sigma(v)N_Y$) and the projectile flux ($J = N_X v$), one can write:

$$r = FJ. \tag{7}$$

In the stellar plasma the product between cross section and particle velocity has to be averaged over the probability $\phi(v)$:

$$\langle\sigma v\rangle = \int_0^\infty \phi(v)v\sigma(v)\mathrm{d}v. \tag{8}$$

It follows that the reaction rate becomes:

$$r = N_X N_Y \langle\sigma v\rangle (1 + \delta_{XY})^{-1}, \tag{9}$$

where δ_{XY} is the Kronecker symbol.

Note that, deriving with respect to time N_X, we obtain the average life time of X interacting with Y:

$$\left.\frac{\mathrm{d}N_X}{\mathrm{d}t}\right|_Y = -\frac{1}{\tau_Y(X)}N_X, \tag{10}$$

with

$$\tau_Y(X) = \frac{1}{N_Y\langle\sigma v\rangle}\,. \tag{11}$$

In the majority of the hydrostatic equilibrium phases, the stellar plasma can be considered as a non-degenerate and non-relativistic gas, therefore the velocity distribution follows the Maxwell-Boltzmann law:

$$\phi(v) = 4\pi v^2\left(\frac{m}{2\pi kT}\right)^{3/2}\exp\left[-\frac{mv^2}{2kT}\right], \tag{12}$$

where v is cm/s, m in amu, T in K and k is the Boltzmann constant, or

$$\phi(E) \propto E\exp\left[-\frac{E}{kT}\right]. \tag{13}$$

In the center-of-mass system, eq. (8) becomes:

$$\langle\sigma v\rangle = \left(\frac{8}{\pi\mu}\right)^{1/2}\frac{1}{(kT)^{3/2}}\int_0^\infty \sigma(E)E\exp\left[-\frac{E}{kT}\right]\mathrm{d}E, \tag{14}$$

where $\mu = m_X m_Y/(m_X + m_Y)$ is the reduced mass in amu. With these assumptions we can re-write eq. (9):

$$r = N_X N_Y\left(\left(\frac{8}{\pi\mu}\right)^{1/2}\frac{1}{(kT)^{3/2}}\int_0^\infty \sigma(E)E\exp\left[-\frac{E}{kT}\right]\mathrm{d}E\right)(1+\delta_{XY})^{-1}. \tag{15}$$

Therefore, the energy coefficient for the $1+2\rightarrow 3+4$ reaction is:

$$\epsilon_{nuc} = \epsilon_{12} + \epsilon_{34} = (r_{12} - r_{34})\frac{Q}{\rho}\,. \tag{16}$$

5 Reaction rates in stellar environments

In order to determine the temperature dependence of the reaction rate one has to know the cross section in the relevant energy range to evaluate the integral in eq. (15). Due to the strong energy dependence of the penetrability of the Coulomb barrier, the astrophysical S factor is usually introduced by the following parametrisation of the cross section,

$$\sigma(E) = \frac{1}{E}\exp[-2\pi\eta]S(E), \tag{17}$$

in terms of the de Broglie wavelength ($\lambda^2 \propto 1/p^2 \propto 1/E$), the s-wave barrier penetration factor (in the approximation valid for $E \ll E_C$) and the slowly varying factor $S(E)$ (MeV barn), which accounts for the nuclear properties of the process.

In the above expression, η is the Sommerfeld parameter: $\eta = \frac{Z_1 Z_2 e^2}{\hbar\nu}$. Substituting this expression for the cross section in eq. (14), we have:

$$\langle\sigma v\rangle = \left(\frac{8}{\pi\mu}\right)^{1/2}\frac{1}{(kT)^{3/2}}\int_0^\infty S(E)\exp\left[-\frac{E}{kT} - \frac{b}{E^{1/2}}\right]\mathrm{d}E, \tag{18}$$

where $b = \frac{(2\mu)^{1/2}\pi e^2 Z_1 Z_2}{\hbar}$.

In those cases in which $S(E)$ can be considered constant in the energy range in which the exponential in the integrand of eq. (18) is significantly larger than zero, the latter shows a maximum (Gamow peak, see fig. 4) in

$$E_0 = \left(bk\frac{T}{2}\right)^{2/3} = 1.22(Z_1^2 Z_2^2 \mu T_6^2)^{1/3}\,\mathrm{keV}, \tag{19}$$

where T_6 is 10^6 K. An estimate of the width of the Gamow peak can be obtained by $\Delta = \frac{4}{3^{1/2}}(E_0 kT)^{1/2}$.

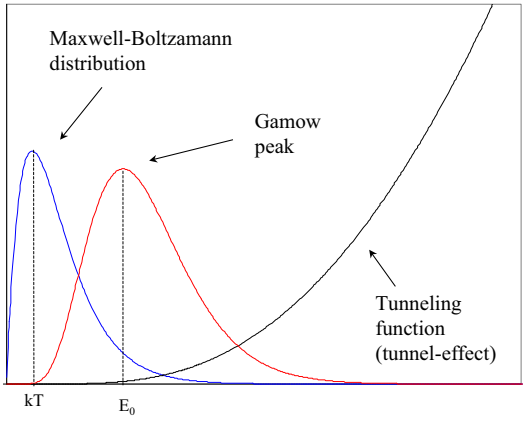

Fig. 4. The dominant energy-dependent functions are shown for nuclear reactions between charged particles.

The above treatment is valid when $S(E)$ can be considered constant across the Gamow peak. A better approximation can be obtained performing a series expansion of the $S(E)$ function around the energy axis origin (the Gamow peak is always lying at very low energies), involving not only the $S(0)$ value, but also the first and, in some cases, the second derivative $S'(0)$ and $S''(0)$, obtained from fits to experimental data (see next section). In all cases the insertion of this expansion of $S(E)$ in eq. (18) and the approximation of the Gamow peak with a Gaussian function including a correction factor [12] leads to an analytic expression of the reaction rate of the kind:

$$\langle \sigma v \rangle = AT^{-2/3} \exp\left[-BT^{-1/3}\right] \sum_{i=0}^{5} \alpha_i T^{i/3}, \tag{20}$$

with the coefficients depending on $S(0)$, $S'(0)$ and $S''(0)$.

The quadratic approximation for $S(E)$ is valid in the non-resonant case, *i.e.* when the contributions to the cross section arising from resonances in the compound nucleus in the relevant energy range are negligible. In this case, the cross section is dominated by direct reaction mechanisms. In the frequent case of radiative capture, *i.e.* the reaction in which the exit channel consists of a photon plus a residual nucleus, the direct capture is a process in which the electromagnetic interaction induces a transition of the target+projectile system in a state in the continuum to a final bound state with a well-defined orbital angular momentum, accompanied by the emission of a γ-ray. The reaction proceeds without the formation of an intermediate (compound nucleus) state, and the partial wave(s) involved, in the incident plane wave expansion, are selected by the selection rules of the relevant electric or magnetic multipole operators.

If, on the other hand, at the excitation energy of the compound system $E_x = E_{cm} + Q$ a virtual unbound state of the compound nucleus exists, the resonant excitation of this state in the entrance channel a and the subsequent decay in the exit channel b is described by the Breit-Wigner equation [12]:

$$\sigma(E) = \pi\lambda^2 \frac{2J_R + 1}{(2J_1 + 1)(2J_2 + 1)} (1 + \delta_{12}) \frac{\Gamma_a \Gamma_b}{(E - E_R)^2 + (\frac{\Gamma}{2})^2}\,, \tag{21}$$

where J_R is the angular momentum of the resonance, J_1 and J_2 those of the projectile and target, E_R is the resonance energy and Γ_a, Γ_b and Γ are the partial and total widths of the resonance. In the case of narrow resonances, *i.e.* when the total width is much smaller than the resonance energy, the integrand in eq. (18) is dominated by the cross section term, and the other terms can be assumed to be a constant equal to the value assumed at $E = E_r$. Moreover, the energy dependence of total and partial widths can be neglected across the resonance, so that the reaction rate can be written as

$$\langle \sigma v \rangle = \left(\frac{2\pi}{\mu kT}\right)^{3/2} \hbar^2 (\omega\gamma)_R \exp\left[\frac{-E_R}{kT}\right], \tag{22}$$

where ω is the statistical weight $\frac{2J+1}{(2J_1+1)(2J_2+1)}(1 + \delta_{12})$, γ the strength of the resonance, which is given by $\gamma = \frac{\Gamma_a \Gamma_b}{\Gamma}$.

The exponential term indicates that at given stellar temperature the reaction rate is dominated by resonances with energy E_R close to kT.

Finally, the case of broad resonances, *i.e.* when the total width is comparable with the resonance energy, can be treated similarly to the non-resonant case, with the difference that the S factor at the Gamow energy can be expressed in terms of the parameters of the resonance contributing with its tail to the cross section. It has to be noted that, in this case, more than one resonance in the vicinity of the Gamow energy, including subthreshold resonances (*i.e.* the tail of a bound state lying slightly below the particle emission threshold), can contribute to the cross section, and interference terms between different amplitudes have to be taken into account.

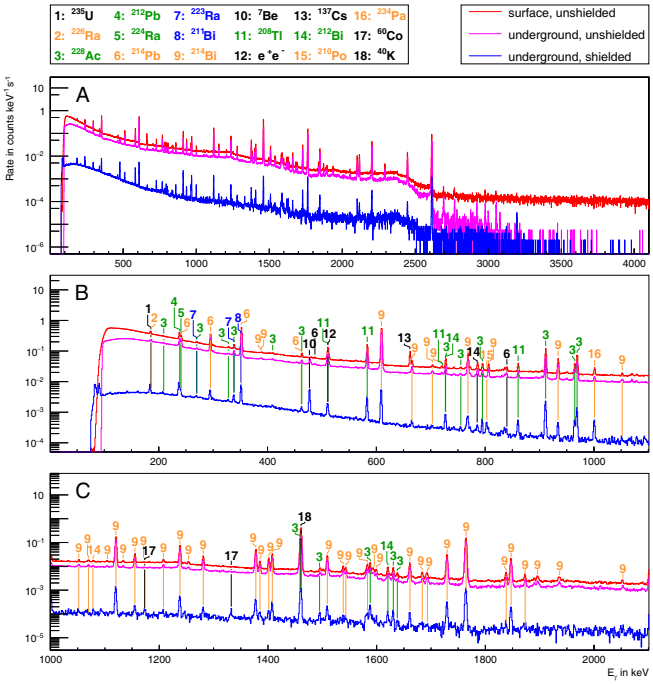

Fig. 5. Background spectra acquired with the same HPGe detector in three different locations: surface unshielded, underground unshielded and underground shielded by 15 cm of lead [3].

6 Features of underground cross section measurements

For a given stellar temperature T, nuclear reactions are taking place mainly inside the Gamow peak. In the case of H-burning typical energies are of the order of tens of keV (for example, about 25 keV for $^{14}\mathrm{N}(\mathrm{p},\gamma)^{15}\mathrm{O}$). Cross sections at the Gamow peak energy are of the order of 10^{-9}–10^{-12} barn corresponding to experimental counting rates ranging from a few events per day to a few events per month under typical laboratory conditions. This means that in realistic experimental conditions, the expected counting rate is prohibitively low and the competition with cosmic background strongly hinders obtaining statistically significant results.

There are three sources of background: cosmic rays, environmental radioactivity and beam target impurity induced nuclear reactions. Each of these sources produces background of a different nature and energy, so that each reaction studied needs special attention in suppressing the relevant background component. A number of techniques have been developed to reduce the background component by improved detector configuration, event identification and background rejection techniques [13,14]. A possible approach uses quite complex apparatuses to optimize the detection efficiency, selectivity and the background suppression. An example is Recoil Mass Separators (RMS) [15–17], in inverse kinematic, that allow one to measure the cross section of radiative capture reactions by means of the detection of the residual nucleus. Gamma coincidence measurements can be added in order to gain informations on the transitions involved in the reaction. On the other hand, low-energy studies of thermonuclear reactions in a laboratory on the earth's surface are hampered predominantly by background effects of cosmic rays in the detectors, leading typically to more than 10 events per hour in common detectors. Conventional passive or active shielding around the detectors can only partially reduce the problem. The best solution is to install an accelerator facility in a laboratory deep underground, similar to the solar neutrino detectors. The first example of this approach has been done in the experimental halls of Laboratori Nazionali del Gran Sasso (LNGS) in Italy. The Gran Sasso Mountain, with an average thickness of 1400 m of rock or 3800 mwe (metre water equivalent) above the laboratory halls, led to a reduction of the muon flux, the most penetrating component of the cosmic rays, by a factor 10^6 compared with the surface, thus providing a low-background environment [18]. Similar approaches are presently developed in USA (CASPAR) and China (JUNA). Thermonuclear reactions induced by charged particles are mainly studied by means of γ-ray or particle spectroscopy. The main sources of natural γ-ray background arise from several sources: *i.e.* radionuclides belonging to the natural radioactive series of uranium and thorium or long-lived natural radionuclides such as ^{40}K. All these radionuclides lead to γ-ray background with signals below $E_\gamma = 3.5$ MeV. In comparison, the γ-ray background above $E_\gamma = 2.6$ MeV is mainly dominated by the effects of cosmic rays in the detectors, *i.e.* muon and neutron-induced events (see fig. 5 top panel). The rock shielding of LNGS leads, in a HPGe γ-ray detector, to about 3 orders of magnitude reduction in the γ-ray background signal above $E_\gamma = 2.6$ MeV (see figs. 5 central and lower panels and fig. 6), *i.e.* the region above natural radioactivity.

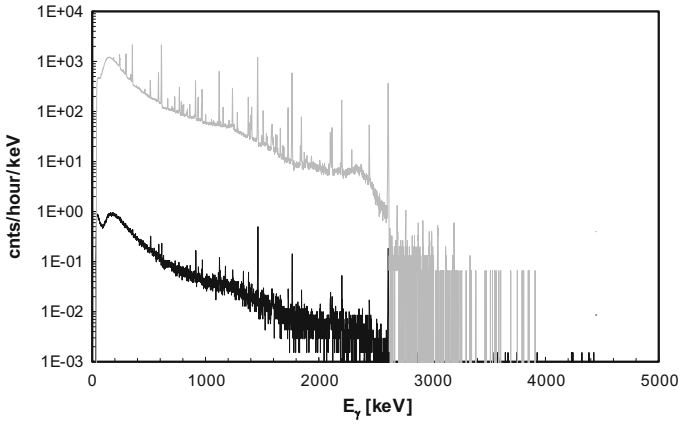

Fig. 6. γ-ray backgrounds as observed with a HPGe detector placed underground (gray line) and with a lead shielding and radon box (black line).

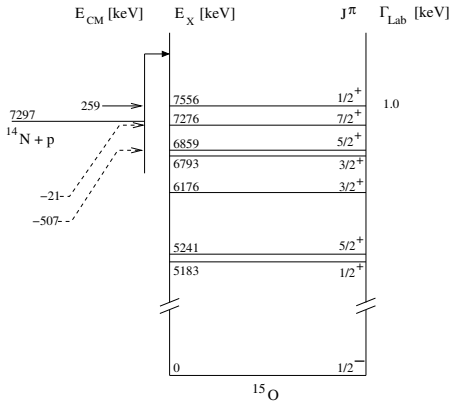

Fig. 7. The level structure of ^{15}O. (Above the ^{14}N(p, γ)^{15}O threshold only relevant states are shown).

Therefore, the advantage of an underground environment is evident for high Q-value reactions, such as ^{14}N(p, γ)^{15}O, ^{15}N(p, γ)^{16}O, or ^{23}Na(p, γ)^{24}Mg, but appears less evident for low Q-value reactions. On the other hand, in a surface laboratory passive shielding, such as lead, can be placed around the detectors but it is limited to a certain thickness. One cannot add further shielding material since cosmic-ray muons interact with the material and create energetic neutrons which, in turn, create γ-rays in the lead. Clearly, this background component is dramatically reduced with the significantly suppressed muon flux in an underground laboratory. An additional γ-ray background component below $E_\gamma = 2.6$ MeV arises due to neutron-induced events. A separate treatment is needed for radon ^{222}Rn, which is a short-lived radioactive gas and a daughter product of the uranium and thorium decay chains. A popular solution to this problem is to house the detector in a box with a small overpressure of flushing nitrogen [19,20,3].

7 Nuclear astrophysics experiments: selected examples of direct measurement

7.1 ^{14}N(p, γ)^{15}O measurement and the age of globular cluster

The ^{14}N(p, γ)^{15}O reaction is the slowest process in the CNO cycle and it is of high astrophysical interest, since its rate influences sensitively the age determination of globular clusters and the solar neutrino spectrum [11]. The capture cross section needs to be known down to $E_0 = 25$ keV (the Gamow peak in core H-burning stars), which is far below the low-energy limit of direct γ-ray measurements A number of measurements of the ^{14}N(p, γ)^{15}O cross section have been carried out over the past 45 years. Figure 7 shows the level scheme of ^{15}O together with some information about the total widths Γ (keV) and the resonance energies E_r in the center-of-mass system. The Q-value of the reaction is 7297 keV [21]. The decay of the resonance at $E_r = 259$ keV (the resonance energy in the center-of-mass system) populates the ground state and the $E_x = 6793$ keV, 6176 keV, and 5183 keV excited states. Each of the excited states decays directly to the ground state of ^{15}O. Schröder *et al.* [22] measured the prompt-capture γ radiation from this reaction in the energy range $E_p = 0.2$ to 3.6 MeV, using both a windowless ^{14}N gas target and implanted ^{14}N solid targets. They found that the reaction mechanism at low energies included contributions from resonant capture at $E_r = 259$ keV, direct capture, and capture from the tail of a sub-threshold resonance at $E_r = -507$ keV (the resonance energy in the center-of-mass system), corresponding to the known $E_x = 6793$ keV state in ^{15}O (see fig. 7).

The analysis of Schröder led to a total astrophysical factor: $S_{\rm tot}(0) = 3.20 \pm 0.54\,{\rm keV\,b}$ [22]. From extrapolation to astrophysical energies, they observed a negligible contribution from capture to the $3/2^-$ state at $E_x = 6176\,{\rm keV}$, and the contributions from capture to the states, at $E_x = 5183\,{\rm keV}$, $5241\,{\rm keV}$, $6859\,{\rm keV}$, and $7276\,{\rm keV}$ account for less than 3% of the total zero-energy $S(E)$-factor. Instead, a significant contribution to the total $S(E)$-factor, about 50%, comes from direct capture to the $E_x = 6793\,{\rm keV}$ state.

The remaining contribution to the total astrophysical factor comes from the transition to the ^{15}O ground state. Transitions to the ^{15}O ground state involve the E1 contributions from the $J^\pi = 1/2^+$ resonance at $E_r = 259\,{\rm keV}$, and the two broader $J^\pi = 3/2^+$ resonances at $E_r = 987\,{\rm keV}$ and $2187\,{\rm keV}$. Several efforts have been invested into improved experimental data and extrapolation technique, by different authors a series of new experiments using direct [23–29], and indirect approaches [30–34], and have been carried out over the last 15 years. A complete and detailed review of the full data available is beyond the aim of the present paper. Hereafter, we would like to present the underground technique to explore the lower energies which measurements represent a huge experimental challenge.

The LUNA Collaboration started in 2000 a new experiment based on two different approaches. First, measurements were performed using a high-resolution HpGe detector in combination with a solid, high purity ^{14}N target to identify the contributions of the different transitions. Then a different setup was used, consisting of a large-volume high-efficiency BGO summing detector in combination with a ^{14}N gas target, in order to extend the measurements of the total cross section of the reaction to an energy as close as possible to the Gamow energy. The goal of the first phase was to study the single γ-transitions and in particular the ground state transition. Therefore a high-resolution HpGe detector was used and it was possible to distinguish the single decays. The price for using a high-resolution germanium detector is the relatively low detection efficiency. Therefore to push the cross section measurements toward lower energies a second phase of the experiment was started using a nearly 4π BGO summing crystal. The absolute efficiency at 7 MeV was about 65%. Due to the non-sufficient energy resolution of the BGO detector it was not possible to have information on the single γ-transitions but the total cross section was measured down to 70 keV. The two different approaches were complementary and both took extreme advantage of the low background laboratory. The resulting reaction rate is lower than a factor 2 from the previous determination [35] for temperature lower than $150 \cdot 10^6\,{\rm K}$ [23,24,27,29] with a average uncertainty of less than 10%. The consequence of the study of $^{14}{\rm N(p,\gamma)^{15}O}$ cross section is the reduction of a factor 2 of solar CNO neutrinos [8] and the increase of the age of globular clusters, using the rate calculated in [24] or [8]. Globular clusters represent the oldest resolved stellar populations [11]. Their age practically coincides with the time elapsed since the epoch of the formation of the first stars in the Universe and provides an independent check of the reliability of cosmological models. Moreover, the age spread in the GC system is a primary indicator of the time scale of the galactic halo formation. Among the various methods to date stellar Clusters, the most reliable and widely adopted is that based on the measurement of the luminosity of the turnoff (*i.e.*, the bluest point in the main sequence). This dating technique requires the knowledge of the Cluster distance, the light extinction along the line of sight and the chemical composition. In addition, a reliable theoretical calibration of the turnoff luminosity-age relation (TOL-A) is needed. This relies on our knowledge of the physical processes of energy generation (*e.g.*, nuclear reactions) and transport (*e.g.*, opacity) taking place in H-burning low-mass stars. The main sequence stars presently observed in globular clusters have masses smaller than that of the Sun. As in the Sun, these low mass stars burn H in the center, mainly through the pp chain. However, towards the end of their life, when the central hydrogen mass fraction becomes smaller than about 0.1, the nuclear energy released by the H burning becomes insufficient and the stellar core contracts to extract some energy from its own gravitational field. Then, the central temperature (and the density) increases and the H burning switches from the pp chain to the more efficient CNO cycle. Thus, the departure from the main sequence is powered by the CNO cycle, whose bottleneck is the $^{14}{\rm N(p,\gamma)^{15}O}$ reaction. The luminosity of the turnoff depends on the rate of this key reaction: the larger the rate, the fainter the turnoff. In contrast, the total lifetime is only marginally affected by a change in the CNO, because it is mainly determined by the rate of the $^1{\rm H(p},e^+,\nu e)^2{\rm H}$. As a consequence, an increase of the CNO rate would imply fainter turnoff points for a given age, or younger ages for a given turnoff luminosity. In conclusion, with the present determination of the reaction rates the main astrophysical consequence is that the age increase of the globular clusters by about 1 Gyear, *i.e.*, about 14 ± 1 Gyears depending by the metallicity of the globular cluster. This value is compatible with the results of WMAP (Wilkinson microwave anisotropy probe) [36], which measuring the fluctuation of the microwave background radiation has accurately measured the fundamental cosmological constants, deriving in the Λ cold dark matter model the age of the Universe in 13.7 ± 0.2 Gyears [11].

7.2 The ^{12}C + ^{12}C measurement

A precise knowledge of the $^{12}{\rm C} + {}^{12}{\rm C}$ reaction rate is of utmost importance to improve our understanding of stellar evolution and nucleosynthesis, since it determines the transition mass between the progenitors of core-collapse and thermonuclear supernovae, determines their outcomes such chemical yields, light curves, and spectral evolution [37,38].

Low energy fusion of $^{12}{\rm C} + {}^{12}{\rm C}$ proceeds mainly through the $^{12}{\rm C}(^{12}{\rm C},\alpha)^{20}{\rm Ne}$ and $^{12}{\rm C}(^{12}{\rm C},{\rm p})^{23}{\rm Na}$ reactions. Successful modelling of carbon burning requires cross sections of these reactions to be known with high accuracy

down $E_{cm} \simeq 1.5\,\mathrm{MeV}$. However, at energies around 2.5 MeV, the reaction yields of these nuclear processes are so small, in the order of few reactions per hour, that their direct measurements are quite challenging [39–41]. In the last 4 decades the $^{12}\mathrm{C}(^{12}\mathrm{C},\alpha)^{20}\mathrm{Ne}$ and $^{12}\mathrm{C}(^{12}\mathrm{C},\mathrm{p})^{23}\mathrm{Na}$ reactions were directly investigated, using both charged-particle and γ-ray spectroscopy, over a wide range of energies, down to about $E = 2.1\,\mathrm{MeV}$. The low counting rates had to confront with severe background issues, stemming from the presence of $^{1}\mathrm{H}$ and $^{2}\mathrm{H}$ contaminations in the targets. As a consequence, the results of the cross section measurements at E lower than 3 MeV are rather uncertain. The extrapolation toward lower energies, needed to make astrophysical predictions, is complicated by the presence of several resonances, the origin of which is not fully understood. Recently, an indirect measurement based on THM method [42] measured the cross section on the whole energy widow of astrophysical interest, showing the presence of several states, which will completely dominate the stellar reaction rate.

To validate these results a direct measurement down to the Gamow energies window is highly requested. The reduced γ-ray background in underground represents the unique location where the carbon fusion reactions can be investigated directly at the relevant astrophysical energy. In the γ-ray spectroscopy experiment one has to detect the transitions from the first excited states in $^{20}\mathrm{Ne}$ ($E_\gamma = 1634\,\mathrm{keV}$) and $^{23}\mathrm{Na}$ ($E_\gamma = 440\,\mathrm{keV}$). These low-energy gammas lie in a region of very high environmental background and at low reaction energies their observation is affected by intense beam-induced background from the $E_\gamma = 2.36\,\mathrm{MeV}$ line from $^{1}\mathrm{H}(^{12}\mathrm{C},\gamma)^{13}\mathrm{N}$ and the $E_\gamma = 3.09\,\mathrm{MeV}$ line from $^{2}\mathrm{H}(^{12}\mathrm{C},\mathrm{p}\gamma)^{13}$. The lowest-energy measurement so far has been performed at the 4 MV Dynamitron tandem at the Ruhr-Universitat Bochum [40].

The data show that the resonance structure extends down to about 2.1 MeV, but the measurements eventually could not continue further down due to too high natural background levels. Therefore, the study of $^{12}\mathrm{C} + {}^{12}\mathrm{C}$ fusion reactions using γ-spectroscopy is an excellent case to be measured in a deep underground laboratory. It has been already mentioned that just by going underground, the γ-ray background above 2.6 MeV is reduced by of about 3 orders of magnitude. Moreover, to reduce the low-energy environmental background radiation, passive shielding around the detector is more effective underground than on the surface, where secondary radiation produced by cosmic ray interactions with the shielding itself acts as a further source of background. We can estimate that 15 cm thick modular lead shielding, as the one used in [3], the improvement in environmental background reduction using the underground lead shield is of more than 2 orders of magnitudes for gamma energies below 2 MeV (see fig. 5).

Additional improvements of the shielding to reduce low energy γ-ray background are possible: flushing the surroundings of the detector with clean nitrogen to remove airborne backgrounds from radon, adding a reduction factor of about another order of magnitude [20]; and using a thicker shielding of about 20 cm made of low intrinsic radioactivity lead, again mounted on rails so that one has easy access to targets when a change is required. This configuration will reduce the gamma background of more than 3 orders of magnitude compared with [40], confirming that deep underground laboratory represents the unique place where it will be possible to directly measure these keys processes down to the Gamow energy window.

8 Conclusion

A complete overview of the experimental Nuclear Astrophysics researches is beyond the aim of this article, since the Nuclear Astrophysics can be considered as transverse field among Nuclear Physics, Astrophysics, and Neutrino Physics. The authors consider this contribution as an interesting starting point for PhD students to discuss the experimental efforts and the prospectives in a such wide variety and diversity topics.

The experimental work described in this paper has been mainly developed in the framework of the LUNA experiments. The authors would like to thank all the members of this international collaboration.

Author contribution statement

All the authors were involved in the preparation of the manuscript. All the authors have read and approved the final manuscript.

Publisher's Note The EPJ Publishers remain neutral with regard to jurisdictional claims in published maps and institutional affiliations.

References

1. R.J. Deboer *et al.*, Rev. Mod. Phys. **89**, 035007 (2017).
2. R.E. Tribble *et al.*, Rep. Prog. Phys. **77**, 106901 (2014).
3. A. Boeltzig *et al.*, J. Phys. G **45**, 025203 (2018).

4. H. Costantini *et al.*, Rep. Prog. Phys. **72**, 086301 (2009).
5. D.C. Clayton, *Principles of Stellar Evolution and Nucleosynthesis* (University of Chicago Press, 1968).
6. G. Gilmore *et al.*, Messenger **147**, 25 (2012).
7. S.W. Stahler, F. Palla, *The Formation of Stars* (Wiley-VCH, Weinheim, 2004).
8. E.G. Adelberger *et al.*, Rev. Mod. Phys. **83**, 195 (2011).
9. H.A. Bethe, Phys. Rev. **55**, 434 (1939).
10. C.F. von Weizsacker, Phys. Z **39**, 633 (1939).
11. G. Imbriani *et al.*, Astron. Astrophys. **420**, 625 (2004).
12. C.E. Rolfs, W.S. Rodney, *Cauldrons in the Cosmos* (University of Chicago Press, 1988).
13. A. Couture *et al.*, Phys. Rev. C **77**, 015802 (2008).
14. R.C. Runkle *et al.*, Phys. Rev. Lett. **94**, 082503 (2005).
15. D. Schürmann *et al.*, Eur. Phys. J. A **26**, 301 (2005).
16. A. Di Leva *et al.*, Phys. Rev. Lett. **102**, 232502 (2009).
17. C. Matei *et al.*, Phys. Rev. Lett. **97**, 242503 (2006).
18. H. Costantini, A. Formicola, G. Imbriani, M. Junker, C. Rolfs, F. Strieder, Rep. Prog. Phys. **72**, 086301 (2009).
19. H.V. Klapdor-Kleingrothaus *et al.*, Nucl. Instrum. Methods A **522**, 371 (2004).
20. A. Caciolli *et al.*, Eur. Phys. J. A **39**, 179 (2009).
21. G. Audi, A.H. Wapstra *et al.*, Nucl. Phys. A **729**, 337 (2003).
22. U. Schröder *et al.*, Nucl. Phys. A **467**, 240 (1987).
23. A. Formicola *et al.*, Phys. Lett. B **591**, 61 (2004).
24. G. Imbriani *et al.*, Eur. Phys. J. A **25**, 455 (2005).
25. R.C. Runkle *et al.*, Phys. Rev. Lett. **94**, 082503 (2005).
26. R.C. Runkle *et al.*, Phys. Rev. Lett. **94**, 082503 (2005).
27. A. Lemut *et al.*, Phys. Lett. B **634**, 483 (2006).
28. D. Bemmerer *et al.*, Nucl. Phys. A **779**, 297 (2006).
29. M. Marta *et al.*, Phys. Rev. C **78**, 022802(R) (2008).
30. A.M. Mukhamedzhanov *et al.*, Phys. Rev. C **67**, 065804 (2003).
31. D. Schürmann *et al.*, Phys. Rev. C **77**, 055803 (2008).
32. S.O. Nelson *et al.*, Phys. Rev. C **68**, 065804 (2003).
33. P.F. Bertone *et al.*, Phys. Rev. Lett. **87**, 152501 (2001).
34. K. Yamada *et al.*, Phys. Lett. B **579**, 265 (2004).
35. C. Angulo *et al.*, Nucl. Phys. A **656**, 3 (1999).
36. C. Bennett *et al.*, Astrophys. J. **583**, 123 (2003).
37. O. Straniero, L. Piersanti, S. Cristallo, J. Phys.: Conf. Ser. **665**, 012008 (2016).
38. B. Leibundgut, Annu. Rev. Astron. Astrophys. **39**, 67 (2001).
39. H.W. Becker *et al.*, Z. Phys. A **303**, 305 (1981).
40. T. Spillane *et al.*, Phys. Rev. Lett. **98**, 122501 (2007).
41. L.R. Gasques *et al.*, Phys. Rev. C **76**, 035802 (2007).
42. A. Tumino *et al.*, Nature **557**, 687 (2018).